

Entwicklung eines adaptierten Astigmatismus-PTV-Verfahrens zur Untersuchung der Mikropartikelsegregation in Taylor-Couette Strömungen

Utilizing an adapted astigmatism PTV-procedure to investigate microparticle segregation in Taylor-Couette flows

Philipp Brockmann¹, Hamid Tabaei Kazerooni^{1,2}, Luca Brandt², Jeanette Hussong¹

¹ AG Lasermesstechnik der Mehrphasenströmungen,
Lehrstuhl für Hydraulische Strömungsmaschinen, Ruhr-
Universität Bochum, Universitätsstr. 150, 44801 Bochum

² SeRC and Linne FLOW Centre,
KTH Mechanics,
SE-100 44 Stockholm, Sweden

Astigmatismus-PTV, Partikeldynamik, Suspensionsströmungen
Astigmatism-PTV, particle dynamics, sheared suspension flows

Abstract

Recently, formation of particle bands is observed for suspension flows of buoyant spherical particles in a horizontally aligned and completely filled Taylor-Couette (TC) system under laminar flow conditions. To investigate the particle dynamics, an astigmatism based PTV method is adapted in the present study. Instead of the particle image itself, we use the aberration of the particle's focal point to reconstruct particle positions and velocities inside the TC gap. We show that the experimental results of particle distributions and velocities for a very dilute suspension are in a good agreement with deterministic approximations of a single particle trajectory in a laminar TC flow.

1 Introduction

The particle-banding, i.e. local band-shaped accumulations of particles, is a well-known phenomenon for suspension of buoyant finite size particles in horizontal rotating drums (Lipson and Seiden (2002)). A similar banding phenomenon was also observed by Tirumkudulu et al. (1999) for neutrally buoyant particles in a partially-filled horizontal Taylor-Couette system. Despite different numerical and experimental studies (Hou et al. (2014), Seiden and Thomas (2011)), the hydrodynamic mechanism responsible for the formation of particle bands is still not fully understood.

We discovered that the particle-banding phenomenon may also segregate buoyant particles, according to their size and density, in a completely filled horizontal Taylor-Couette system. The aim of the present study is to investigate the segregation behavior of particles in such flows. To this end, the information of the particle location and displacement inside the Taylor-Couette gap is required. Different optical measurement techniques such as stereo and tomographic PIV (Kim et al. 2012) are proposed in literature to extract the information of out-of-plane position and velocity of a particle. However, if particle images are distorted due to aberrations depending on the camera view and particle location itself, an extensive calibration

procedure will be required. Furthermore, cross-correlation based velocimetry techniques require high particle image densities which are not given in the present system (Wereley and Meinhart 2010).

Another approach is to employ defocusing techniques in which defocused particle images taken by one camera are used to determine the out-of-plane velocity component. Stolz and Köhler (1994) used the size of particle images to determine the location and consequently the 3D displacement of tracer particles. Kao and Verkman (1994) showed that using a weak cylindrical lens in front of the camera causes astigmatism which deforms the circular shape of particle images to an ellipsoid. Indeed, the position of particles with respect to the focal plane of a camera can be obtained by the orientation (horizontal or vertical) of the major axis of the ellipsoid. This has been utilized for the so-called Astigmatism Micro-Particle Tracking Velocimetry (A- μ PTV) method that has been developed and applied successfully by different groups in the last years (Cierpka et al. 2010 and 2012, Rossi and Kähler 2014, Liu et al. 2014). Up to date, A- μ PTV is mainly used to explore the fluid velocity field by tracking the motion of small neutrally buoyant tracers dispersed in a flow.

In the present study, we extend A- μ PTV technique to investigate the behavior of finite-size ($\geq 100 \mu\text{m}$) spherical particles in a narrow gap Taylor-Couette flow. The main difference with previous works is that particles are illuminated in bright-field mode, thereby acting as ball lenses that yield a focal point of light rays passing through the particle. The astigmatism induced shape change of this light ray bundle in the image plane (hence referred to as “focal image”) is very sensitive to the particle’s out-of-plane position. While nearly no skewing of the particle image shape itself is observed, the out-of-plane particle position and displacement is deduced from the “focal image”. The combination of nearly undistorted particle silhouettes and the sensitive behavior of the focal image facilitates a measurement procedure which is robust against overlapping particles and yields high accuracy at the same time.

To reconstruct the particle positions at different positions along the gap, a calibration function is derived, which describes the aspect ratio of the focal image as function of the particle’s out-of-plane position. First, the calibration measurements are carried out for different particle sizes located at the inner and outer cylinders. Next, using the calibration function, particle distributions and velocities are determined at different circumferential positions along the gap. The results are in a good agreement with deterministic approximations of a single particle trajectory in a laminar TC flow (Schröder et al. 2017).

The present work sets the framework to study particle banding phenomena in narrow TC flows as recently observed. However, investigating the underlying hydrodynamic principles of this phenomenon is beyond the scope of this paper and will be part of future studies.

2 Experimental Setup

Figure 1 shows schematic drawing of the experimental set-up. The Taylor-Couette system consists of two horizontally aligned concentric glass cylinders with a gap width of 1 mm. The inner cylinder can be rotated while the outer one is stationary. The images are taken by a CCD camera (La-Vision Imager Intense, 1376x1040 pixels) equipped with a microscope (Nikon Cfi60) with 10X magnification. The field of view is 0.88 mm x 0.66 mm. The camera is flexible to move in radial, azimuthal and axial direction with respect to the TC apparatus. The light beam emitted from a dual-cavity Nd:YAG laser (New Wave Solo III-15, $\lambda=532 \text{ nm}$) propagates inside the inner cylinder along its rotation axis where a red fluorescent plate is mounted in order to produce bright-field background illumination. The light source is adjustable in azimuthal and axial direction.

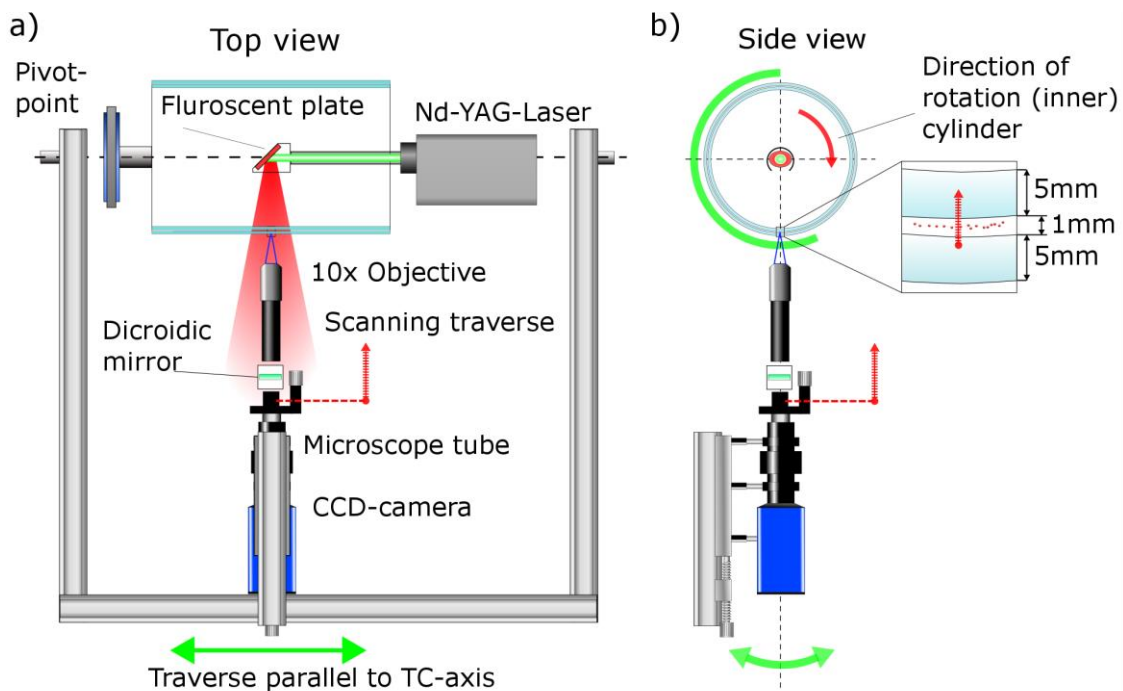


Figure 1: a) Experimental set-up with Taylor-Couette cell and optical system displayed in top view. b) Side view of the experimental setup.

3 Evaluation procedure

Figure 2 shows the measurement principle applied to the Taylor-Couette flow. Here, the outer cylinder acts as cylindrical lens inducing an astigmatism effect to the focal image based on the relative distance between the in-focus planes of the system hence on denoted as F_{xz} and F_{yz} . In fact, the shape of the particle focal image is circular when it is located in the middle of both in-focus planes and it deforms to a vertically or horizontally aligned ellipsoid when the particle's focal point shifts closer to F_{xz} or F_{yz} , respectively. To reconstruct the actual out-of-plane particle location based on the focal image, the spacing between the real location of the particle and its focal point has to be determined. Therefore, a calibration function is required to reconstruct the absolute particle position inside the fluid gap.

Several measurements are performed with PMMA particles (MicroParticles GmbH) of $d=101$, 148 and $196 \mu\text{m}$ particle diameter. Using an automatic traverse mounted on the camera, a wall-attached particle is scanned with $1 \mu\text{m}$ steps over a range of $800 \mu\text{m}$ so that the change of the focal image aspect ratio is fully captured. Figures 3a)-d) show the evolution of the corresponding focal image of the particle with $d=196 \mu\text{m}$.

To determine the image in which particles appear focused, the Tenengrad variance algorithm (Pertuz et al. 2013), is applied to four regions of interest at the edge of the particle images as indicated in Figs. 3e) and f). To find the location of the focal point of the particle, images are binarized and the aspect ratio of the major and minor axis of the ellipsoid are determined.

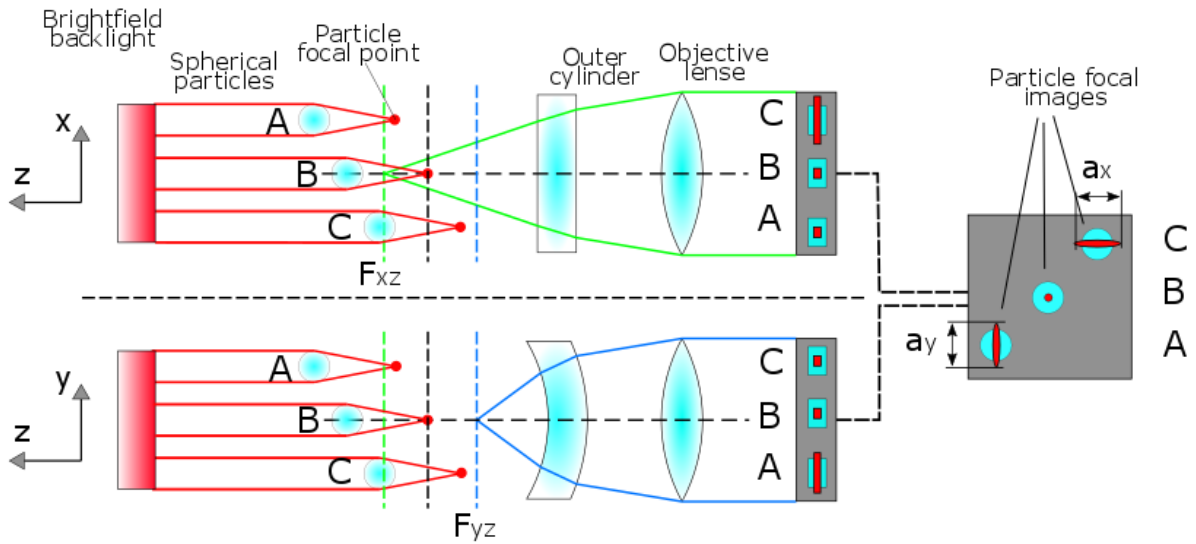


Figure 2: Illustration of the astigmatism-based PTV measurement technique adapted for measurements in an annular gap flow.

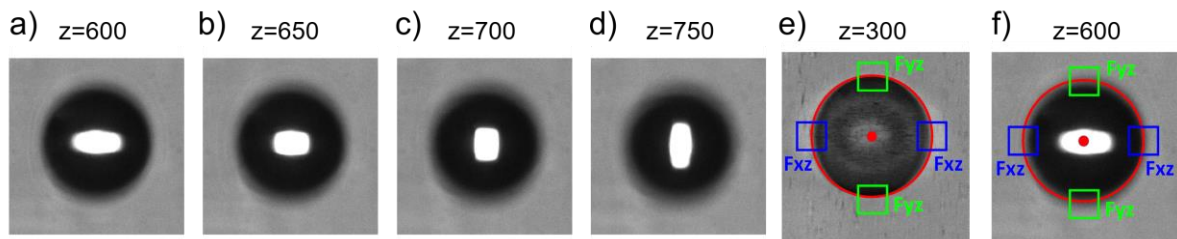


Figure 3: a - d) Evolution of the aspect ratio of the focal image of a particle with $d=196 \mu\text{m}$ located at the inner cylinder. e) and f) The maximum values of the relative focus in the highlighted rectangles are chosen to determine the location of the F_{xz} and F_{yz} planes.

4 Results

4.1 Calibration Curve

Figure 4 shows the evolution of the relative particle focus where the gradient of grey value at the particle rim within the region of interests (see Fig. 3 e) and f)) assume to be maximum at the in-focus planes F_{xz} and F_{yz} . Furthermore, in Fig. 3, the aspect ratio a of the focal image is plotted as obtained from the prescribed scanning procedure. The calibration measurement is performed for particles with $d=101 \mu\text{m}$ located at the inner (Fig.4a) and the outer cylinder (Fig.4b), respectively.

It can be seen, that for the particle at the inner cylinder (Fig. 4a), the distance between the focal planes ($F_{xz}-F_{yz}$) as well as the evolution of the aspect ratio (black curve) differs from the same particle at the outer cylinder (Fig. 4b) due to a different spacing between objective and outer cylinder wall. Furthermore, the evolution of the aspect ratio is different for the same reason.

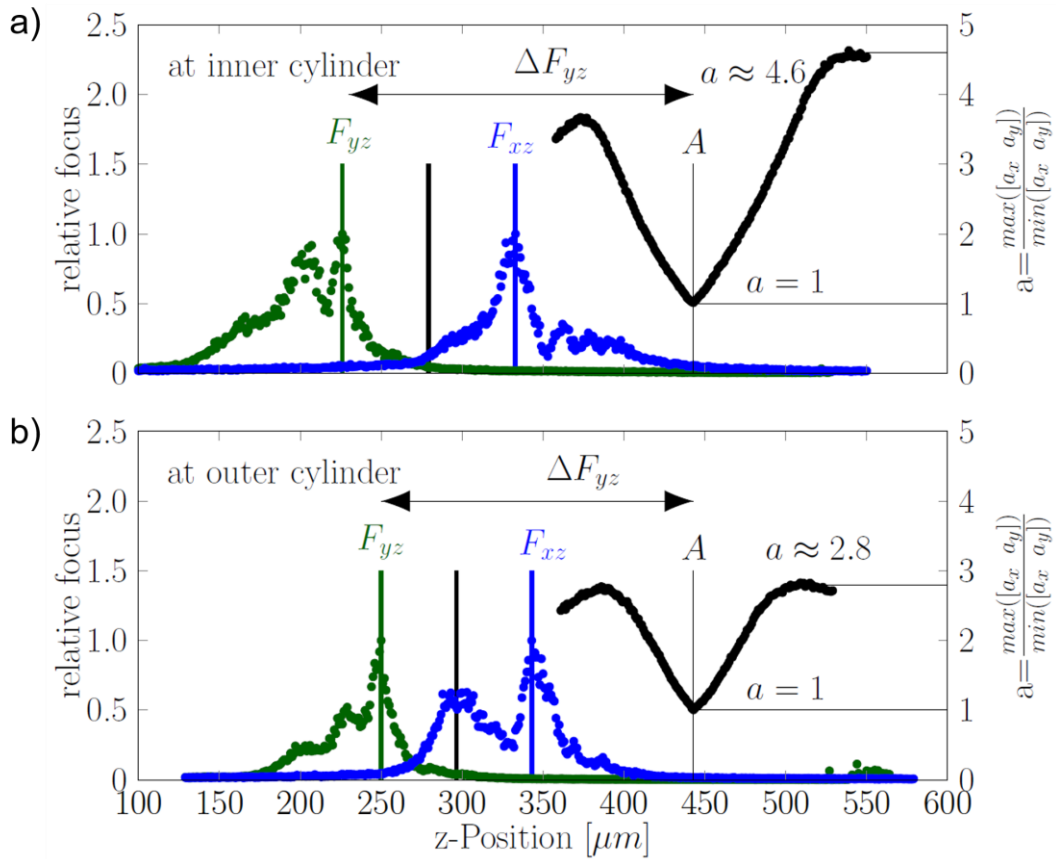


Figure 4: Calibration measurements for a PMMA particle with $d=101 \mu\text{m}$ located at (a) the inner and (b) the outer cylinder. Evolution of the relative particle focus ($150 < z < 400$) and the evolution of the aspect ratio of the focal image ($350 < z < 550$) as function of z-position inside the annular gap.

Figure 5 displays the distance between the focal point and the focal plane F_{yz} for three different particle diameters. Eight measurements were performed for each particle diameter at the inner and the outer cylinder. As the spacing ΔF_{yz} scales linearly with the particle diameter, calibration results gained for the present set-up may be easily transferred to other particle diameters in the future.

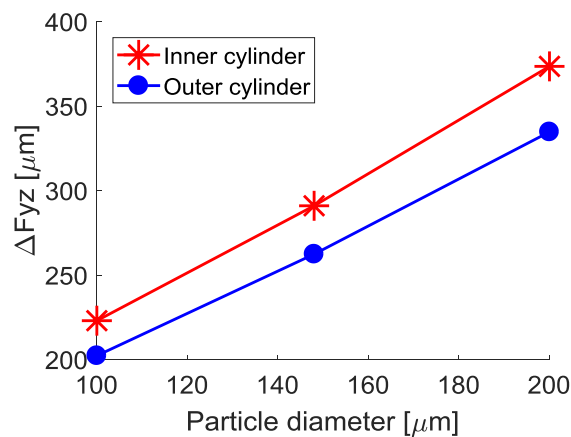


Figure 5: Distance between F_{yz} and the focal image (where aspect ratio = 1) with respect to the particle size

However, the distance between the Fyz plane and the focal image as well as the behavior of the aspect ratio change when a particle moves in radial direction across the fluid gap. Therefore, the main challenge is to generate a calibration function that is valid for every particle and camera position between inner and outer cylinder. For this, measured data of the aspect ratio are superimposed as displayed in Fig 6 a) and b) (black and grey curves) for $d=196 \mu\text{m}$ and $d=101 \mu\text{m}$, respectively. These result from the ratio of the axis (a_x and a_y) of the ellipsoidal focal image (green and blue curve). In the range where the aspect ratio values overlap, a polynomial function is fitted which can be used as calibration function.

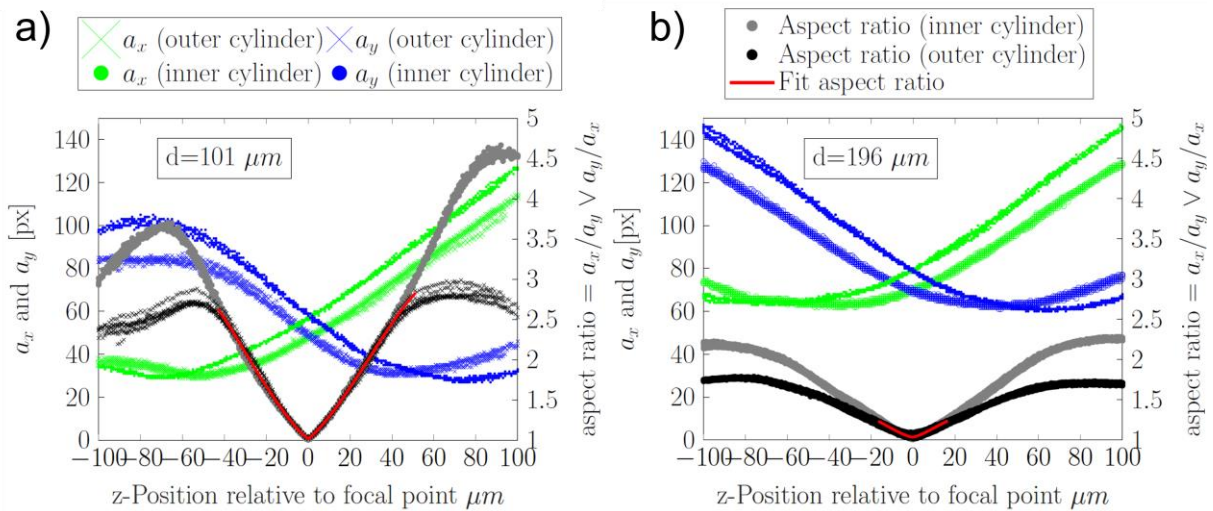


Figure 6: Superimposed measurements of the axis length (a_x and a_y) and the aspect-ratio of the focal image for: a) $d=101 \mu\text{m}$, b) $d=196 \mu\text{m}$ PMMA particle. The red line is polynomial fit, i.e. calibration function.

As it is mentioned before, the distance between particle center and focal point ΔFyz depends on the particle position in the gap. Hence, to reconstruct the position of the particle an iterative calculation procedure is required during which ΔFyz is linearly interpolated based on measurement data. An in-house PTV-Code (Matlab) is developed to evaluate particle velocities and distributions. For this, a double frame image is binarized and the particle centers are determined from the centroids of the binarized focal points. In the next step, the out of plane position of each focal point is determined by its aspect ratio using the calibration function. The particle velocity is calculated by subtracting the coordinates of the best matching, i.e. closest particles of two frames, and then dividing the distance by the time delay Δt between the two frames. In the last step, the absolute position of the particles in the gap is computed.

4.2 Validation measurements

The experimental results presented in this section are based on the calibration function for particles with $d=101 \mu\text{m}$ (Fig 7b). To validate the measurement procedure, particle velocities and particle distributions were measured and compared to a deterministic approximation. The rotation rate was set to 18.5 rpm and particles with $d=101 \mu\text{m}$ diameter were used. The scanning procedure was applied to position 1 and position 2 which are depicted in Fig 7a) where particles are expected to exhibit the maximum and the minimum velocity within the annular gap. At both positions, the gap was scanned in steps of $10 \mu\text{m}$ with 200 double

frame images recorded at each step. The system was in rotation for 24 hours prior to the measurement to achieve stationary conditions.

Corresponding radial particle distributions (blue bar charts) and velocities (red dots) inside the 1 mm annular fluid gap are displayed in Fig 7b). At position 1, the experimental results show that the highest probability of finding particles occurs at $z=54 \mu\text{m}$. This result is in a good agreement with value of $z=50.5 \mu\text{m}$ (particle touches the inner wall) obtained by the deterministic approximation for a single particle at this rotation rate. In addition, the measured velocity for particles close to the inner cylinder $v=0.1097 \text{ m/s}$ is consistent with the result obtained for a single buoyant particle $v=0.1136 \text{ m/s}$ using the deterministic approximation.

At position 2, the highest probability of finding particles was found at $z=945 \mu\text{m}$ experimentally. This is also in a good agreement with $z=949.5 \mu\text{m}$ (particle touches the outer wall) predicted by the deterministic approximation. Corresponding averaged particle velocities of $v=0.00332 \text{ m/s}$ and $v=0.0049 \text{ m/s}$ are obtained via measurement and numerical simulation, respectively.

It should be mentioned that the deterministic approximation only accounts for single-particle dynamics. However, experiments showed that the local concentration of particles increases significantly at position 1 and 2. Indeed, particle interactions play a role at these locations. Particle cloud behavior is observed at position 2 which results in the increase of particle sedimentation velocities compared to the single particle case.

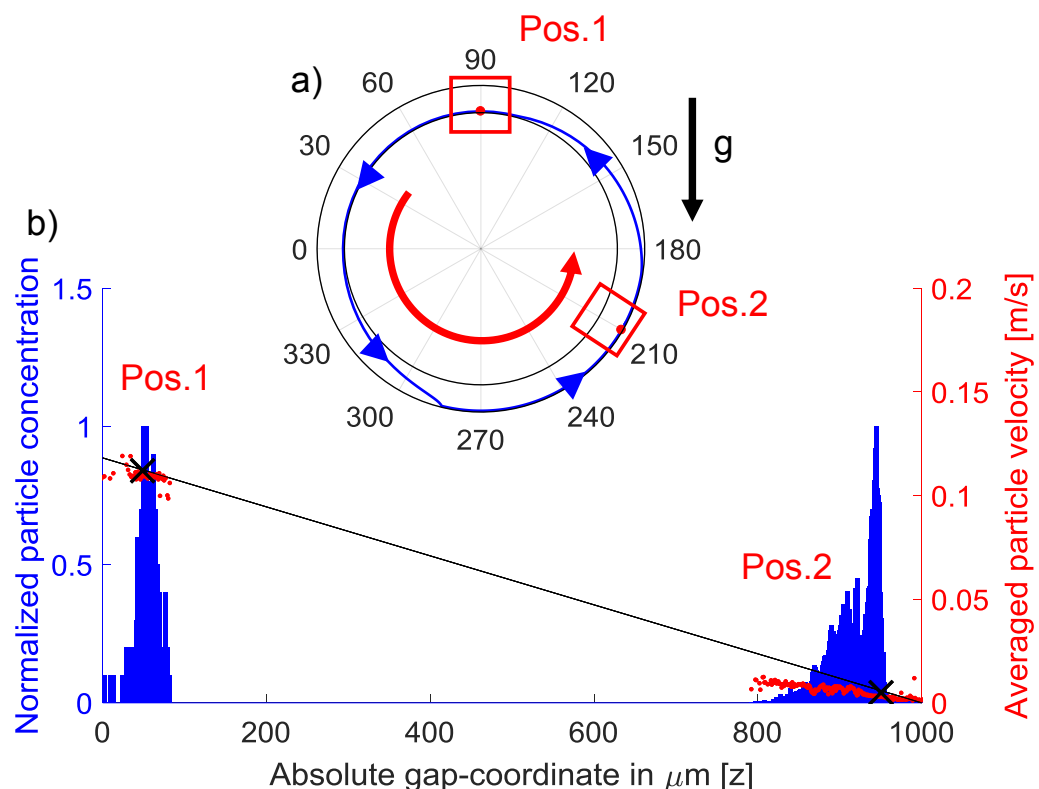


Fig 7: a) Positions (Pos.1 and Pos.2) where the measurements were carried out. b) Probability of particle distribution normalized by absolute number of particles together with the averaged particle velocities. Blue bar charts show experimental results for probability of particle distribution while red dots present the particle velocities. Black cross symbols are the results of numerical simulation for a single buoyant particle (deterministic approximation).

|

5 Conclusion and Outlook

In the present paper, a calibration procedure for an adapted astigmatism based PTV technique is presented to investigate flows in cylindrical systems. Here, particles act as ball lenses and the out-of-plane position is encoded from the aspect ratio of their focal images. In fact, in the present system, the astigmatism induced by the curvature of the outer cylinder of Taylor-Couette apparatus is utilized to reconstruct the out-of-plane position of particles. Hence, no additional cylindrical lens is required here.

Obtaining a proper calibration function is a challenging task due to the fact that the aspect ratio of the focal image shows different behavior for a particle located at the inner and outer cylinder. Furthermore, the distance between the focal point and center of the particle changes along the gap. From the measurements, a region of overlapping curves for the aspect ratio at the inner and outer cylinder was identified in a range of approximately 80 μm for the particle with $d=101 \mu\text{m}$. A polynomial was fitted to this overlapping region and used as calibration function. Using this calibration function, $\mu\text{A-PTV}$ was successfully applied to a test case of very dilute suspension. The results were consistent with the data obtained numerically for the behavior a single particle in a laminar Taylor-Couette flow.

In the future, a generalized calibration function will be utilized to study particle banding phenomena in a completely filled horizontal Taylor-Couette system.

Literature

- Lipson, S. G., & Seiden, G. (2002).** Particle banding in rotating fluids: a new pattern-forming system. *Physica A: Statistical Mechanics and its Applications*, 314(1), 272-277.
- Tirumkudulu, M., Tripathi, A., & Acrivos, A. (1999).** Particle segregation in monodisperse sheared suspensions. *Physics of fluids*, 11(3), 507-509.
- Hou, S., Pan, T. W., & Glowinski, R. (2014).** Circular band formation for incompressible viscous fluid-rigid-particle mixtures in a rotating cylinder. *Physical Review E*, 89(2), 023013.
- Seiden, G., & Thomas, P. J. (2011).** Complexity, segregation, and pattern formation in rotating-drum flows. *Reviews of Modern Physics*, 83(4), 1323.
- Kim, H., Westerweel, J., & Elsinga, G. E. (2012).** Comparison of Tomo-PIV and 3D-PTV for microfluidic flows. *Measurement Science and Technology*, 24(2), 024007.
- Wereley, S.T. and Meinhart, C.D (2010).** Recent advances in micro-particle image velocimetry. *Annual Review of Fluid Mechanics*, 42, pp.557-576.
- Stolz, W. and Köhler, J. (1994).** In-plane determination of 3D-velocity vectors using particle tracking anemometry (PTA). *Experiments in fluids*, 17(1), pp.105-109.
- Kao, H.P. and Verkman, A.S. (1994).** Tracking of single fluorescent particles in three dimensions: use of cylindrical optics to encode particle position. *Biophysical journal*, 67(3), pp.1291-1300.
- Cierpka, C., Segura, R., Hain, R. and Kähler, C.J., (2010).** A simple single camera 3D3D velocity measurement technique without errors due to depth of correlation and spatial averaging for microfluidics. *Measurement Science and Technology*, 21(4), p.045401.
- Cierpka, C. and Kähler, C.J. (2012).** Particle imaging techniques for volumetric three-component (3D3C) velocity measurements in microfluidics. *Journal of visualization*, 15(1), pp.1-31.
- Rossi, M., Segura, R., Cierpka, C., & Kähler, C. J. (2012).** On the effect of particle image intensity and image preprocessing on the depth of correlation in micro-PIV. *Experiments in fluids*, 52(4), 1063-1075.
- Liu, Z., Speetjens, M.F., Frijns, A.J. and van Steenhoven, A.A. (2014).** Application of astigmatism $\mu\text{-PTV}$ to analyze the vortex structure of AC electroosmotic flows. *Microfluidics and nanofluidics*, 16(3), pp.553-569.
- Schröer K. et al. (2017).** Dilute suspensions in annular shear flow under gravity: simulation and experiment, *Powders and Grains 2017*, Montpellier France (accepted, to be published)